Closecoupling calculations on the H+BrH→HBr+H reaction in three dimensions

D. C. Clary

Citation: J. Chem. Phys. **83**, 1685 (1985); doi: 10.1063/1.449355
View online: http://dx.doi.org/10.1063/1.449355
View Table of Contents: http://jcp.aip.org/resource/1/JCPSA6/v83/i4
Published by the AIP Publishing LLC.

Close-coupling calculations on the H + BrH→HBr + H reaction in three dimensions

D. C. Clary
University Chemical Laboratory, Lensfield Road, Cambridge CB2 1EW, United Kingdom

(Received 7 January 1985; accepted 21 February 1985)

Close-coupling calculations on the H + BrH($v = 0, j$)→HBr($v = 0, j'$) + H reaction in three dimensions are reported. Cross sections have been computed for an energy range sufficient to give a converged rate constant at room temperature. The results are used to test the accuracy of sudden approximations and a variational transition state theory with tunneling correction. It is found that these approximate theories slightly overestimate the reaction rate constant.

I. INTRODUCTION

The accurate calculation of rate constants for three-dimensional ($3D$) chemical reactions from given potential energy surfaces remains one of the major problems confronting molecular collision theory. Quantum effects such as tunneling are known to be of vital importance for many reactions, yet the only accurate quantum scattering computations which have been carried out to date on a $3D$ reaction are those for H + H_2→H_2 + H (Refs. 1–3). Accurate quantum results on $3D$ reactions more complicated than this are a vital requirement for testing the reliability of approximations, such as transition state and classical trajectory techniques, which can be applied to a wide range of reactions. Furthermore, results obtained in recent molecular beam experiments suggest that quantum resonances are important in the F + H_2 reaction,[4] and accurate $3D$ quantum calculations are needed to confirm this finding. Given the continuing improvements in *ab initio* methods for calculating potential surfaces of chemical reactions, the ability to test the accuracy of experimental rate constant data for some simple atom + diatom reactions seems a real possibility if only tractable $3D$ quantum reactive scattering methods can be developed.

Although "exact" $3D$ quantum scattering calculations have only been performed on the H + H_2 reaction, several quantum approximations have been applied to more complicated reactions.[5] These include the centrifugal sudden (coupled states) approximation (CSA),[6–10] the infinite order sudden approximation (IOSA),[5,11–17] the distorted wave Born method,[18–29] a technique which uses a combination of the energy sudden approximation (ESA) for the entrance channel, and the CSA for the exit reaction channel[30–33] (the ESA-CSA method) and various methods which modify one-dimensional dynamics to model $3D$.[34–40] Furthermore, variational transition state theories have also shown much promise recently.[41,42] In the absence of "exact" results for reactions beyond H + H_2 the accuracy one can expect from these approximations remains uncertain.

Here we report $3D$ close-coupling (CC) calculations on the reaction

$$\mathrm{H} + \mathrm{BrH}\,(v = 0, j) \rightarrow \mathrm{HBr}\,(v = 0, j') + \mathrm{H}.$$

In these computations, we apply no sudden or decoupling approximations to the solution of the $3D$ close-coupled equations for the entrance and exit reaction channel. In matching the wave function solutions between entrance and exit reaction channels, we assume an infinitely heavy mass for the central atom, which should be very accurate for the H + BrH reaction. Furthermore, we neglect the reaction occurring in the abstraction channel (H + HBr→H_2 + Br). This should be a highly accurate procedure because there is a very strong bending potential away from the favored collinear geometry[31] and the abstraction and exchange reactions should not be strongly coupled at the reaction temperatures considered here (room temperature and below).

We use our CC results to test the accuracy of approximate theories. These include an extended variational transition state theory with semiclassical transmission coefficients, and the ESA-CSA and IOSA methods, in which sudden approximations are used to decouple the close-coupled equations.

Calculations on the H + BrH reaction are of experimental relevance because rate constant[43] and molecular beam measurements[44] have been made on the closely related D + BrH→DBr + H reaction and the vibrationally excited H + BrH(v)→BrH + H reaction could be an important quenching process in the HBr laser.[45] We emphasize, however, that the main goal of the present calculation is to obtain accurate quantum-dynamical results for an assumed potential energy surface, and since this surface (although being of realistic form) is quantitatively uncertain, comparison to experiment must be treated with caution.

Section II describes the methods used in the present CC calculations while Sec. III gives numerical details of the computations. Section IV presents CC calculations of integral reaction cross sections and rate constants for the H + BrH reaction and compares these results with those obtained using the ESA-CSA, IOSA, and transition state methods. Conclusions are in Sec. V.

II. METHOD

A. Coordinates

The entrance and exit reaction channels are denoted by α and β, respectively. In a given reaction channel γ, the diatomic internuclear distance vector in space-fixed coordinates is $\bar{\mathbf{r}}_\gamma$ and the vector joining the attacking atom to the center of mass of the diatomic molecule is $\bar{\mathbf{R}}_\gamma$. The angle between $\bar{\mathbf{r}}_\gamma$ and $\bar{\mathbf{R}}_\gamma$ is θ_γ. The mass-scaled coordinates

$$\mathbf{R}_\alpha = \bar{\mathbf{R}}_\alpha,\ \mathbf{r}_\alpha = (\mu'_\alpha/\mu_\alpha)^{1/2}\bar{\mathbf{r}}_\alpha,$$
$$\mathbf{R}_\beta = (\mu_\beta/\mu_\alpha)^{1/2}\bar{\mathbf{R}}_\beta,\ \mathbf{r}_\beta = (\mu'_\beta/\mu_\alpha)^{1/2}\bar{\mathbf{r}}_\beta, \quad (1)$$

are defined, where μ'_γ is the reduced mass of the diatomic

 0021-9606/85/161685-08$02.10

molecule and μ_γ is the reduced mass of the collisional system. In this system of coordinates, the Hamiltonian for the arrangement channel can be written in space-fixed coordinates (denoted xyz) by

$$H_\gamma = -\frac{\hbar^2}{2\mu_\alpha}\frac{1}{R_\gamma}\frac{\partial^2}{\partial R_\gamma^2}R_\gamma - \frac{\hbar^2}{2\mu_\alpha}\frac{1}{r_\gamma}\frac{\partial^2}{\partial r_\gamma^2}r_\gamma + \frac{\ell_\gamma^2}{2\mu_\alpha R_\gamma^2} + \frac{\mathbf{j}_\gamma^2}{2\mu_\alpha r_\gamma^2} + V(R_\gamma, r_\gamma, \theta_\gamma), \tag{2}$$

where ℓ_γ^2 is the orbital angular momentum operator associated with the angular motion of the scattering atom, $\mathbf{j}_\gamma^2$ is the rotational angular momentum operator and V is the potential energy surface. It is necessary to solve the Schrödinger equation,

$$(H_\gamma - E_{\text{Tot}})\Psi_\gamma^{JM} = 0, \tag{3}$$

where E_{Tot} is the total energy and J is the total angular momentum of the three-body system, with projection quantum number M along the z axis.

It is convenient to use a set of body-fixed coordinates[46] denoted by XYZ for channel γ. These are obtained from xyz by rotating through the Euler angles $(\bar{\alpha},\bar{\beta},0)$ so that the resulting Z axis points along $\mathbf{R}_\gamma$ and the Y axis is in the xy plane. With these coordinates, it is appropriate to replace ℓ_γ^2 in Eq. (2) by $|\mathbf{J}-\mathbf{j}_\gamma|^2$, where $\mathbf{J}$ is the total angular momentum operator.

A curvilinear coordinate system is used[47,48] to describe the reaction. Polar coordinates (u_γ, v_γ), with turning center parameters (R_γ^*, r_γ^*) are employed in the strong interaction region, while the usual "Cartesian" coordinates are used for the weakly interacting region. In the polar region we have

$$\begin{aligned} R_\gamma &= R_\gamma^* - \eta_\gamma\sigma_\gamma \sin\bar{\theta}_\gamma \\ r_\gamma &= r_\gamma^* - \eta_\gamma\sigma_\gamma \cos\bar{\theta}_\gamma \\ \bar{\theta}_\gamma &= \pi/2 - \epsilon_\gamma - u_\gamma/\sigma_\gamma \\ \eta_\gamma &= 1 + v_\gamma/\sigma_\gamma, \end{aligned} \tag{4}$$

where v_γ represents a local vibrational coordinate and u_γ is identified with translational motion. At $\omega_\gamma = 0$, the angle θ_γ must satisfy

$$\theta_\alpha + \theta_\beta = \theta_s, \tag{5}$$

where θ_s is the skew angle for the reaction channel.[48] The polar coordinates defined above match smoothly with the Cartesian coordinates

$$\begin{aligned} u_\gamma &= \sigma_\gamma(\pi/2 - \epsilon_\gamma) + R_\gamma - R_\gamma^*, \\ v_\gamma &= r_\gamma^0 - r_\gamma, \end{aligned} \tag{6}$$

where r_γ^0 is the mass-scaled equilibrium internuclear distance of the diatomic molecule.

B. Close-coupled equations

In the Cartesian region, the wave function Ψ_γ^{JM} is expanded in the close-coupled form

$$\Psi_\gamma^{JM} = \sum_{nj\Omega} f_{nj\Omega}^{JM}(u_\gamma) g_n(v_\gamma) \left[\frac{(2J+1)}{4\pi}\right]^{1/2} D_{M\Omega}^{J*}(\bar{\alpha},\bar{\beta},0) \times Y_{j\Omega}(\theta_\gamma,\phi_\gamma)/(r_\gamma R_\gamma), \tag{7}$$

where f is a "translational" function and g is a vibrational function which is an eigensolution of

$$\left[-\frac{\hbar^2}{2\mu_\alpha}\frac{d^2}{dv_\gamma^2} + V^0(u_\gamma^i, v_\gamma)\right] g_n(v_\gamma) = E_n g_n(v_\gamma), \tag{8}$$

where u_γ^i is a chosen value of u_γ. Furthermore,

$$D_{M\Omega}^{J*}(\bar{\alpha},\bar{\beta},0)$$

is a Wigner rotation function (in the notation of Rose[49]). Also $Y_{j\Omega}(\theta_\gamma,\phi_\gamma)$ is a spherical harmonic[49] and $(\theta_\gamma,\phi_\gamma)$ are the spherical polar angles of $\mathbf{r}_\gamma$ in the body-fixed coordinate system. Note that j is a rotational quantum number and Ω is the projection of both $\mathbf{j}_\gamma$ and $\mathbf{J}$ along the body-fixed Z axis. Substitution of the CC expansion (7) into the Schrödinger equation (3), multiplication on the left by

$$g_{n'}(v_\gamma)\left[\frac{(2J+1)}{4\pi}\right]^{1/2} D_{M\Omega'}^{J}(\bar{\alpha},\bar{\beta},0) Y_{j'\Omega'}^*(\theta_\gamma,\phi_\gamma),$$

and integration over $(v_\gamma,\bar{\alpha},\bar{\beta},\theta_\gamma,\phi_\gamma)$ gives a set of coupled equations in f. These equations have been discussed in detail by, for example, Schatz and Kupperman[50] and will not be repeated here.

In the polar region, the close-coupling expansion is of the same form as Eq. (7) with the additional feature that the scaling factor $(\eta_\gamma)^{1/2}$ multiplies the expansion.[51] The close-coupling equations obtained from this are

$$\frac{d^2}{du_\gamma^2}\mathbf{f}^{\gamma J}(u_\gamma) = \mathbf{A}^{\gamma J}\mathbf{f}^{\gamma J}(u_\gamma), \tag{9}$$

where

$$\begin{aligned} A_{n'j'\Omega' njn}^{\gamma J} &= (3/4\sigma_\gamma^2)\delta_{n'j'\Omega',nj\Omega} + 2\mu_\alpha/\hbar^2[\tfrac{1}{2}\{E_n + E_{n'}\} - E_{\text{Tot}}]\langle g_{n'}|\eta_\gamma^2|g_n\rangle \\ &\times\delta_{j'\Omega',j\Omega} + \langle g_{n'}|\eta_\gamma^2\{[J(J+1)+j(j+1)-2\Omega^2]R_\gamma^{-2} \\ &+ j(j+1)r_\gamma^{-2}\}\delta_{j'\Omega',j\Omega} - ([J(J+1)-\Omega(\Omega\pm1)][j(j+1)-\Omega(\Omega\pm1)])^{1/2} \\ &\times R_\gamma^{-2}\delta_{j'\Omega',j(\Omega\pm1)}|g_n\rangle + 2\mu_\alpha/\hbar^2\langle g_{n'}Y_{j'\Omega'}|\eta_\gamma^2[V(u_\gamma^i,v_\gamma,\theta_\gamma) - V^0(u_\gamma^i,v_\gamma)]|g_nY_{j\Omega}\rangle\delta_{\Omega',\Omega}. \end{aligned} \tag{10}$$

There are a variety of methods available for the numerical solution of the close-coupled equations. We use the R matrix propagation method of Light and Walker, which is fully described in Ref. 48.

C. Wave function matching

Arrangement channel R matrices are obtained, which are denoted $\mathbf{R}_\gamma$ and which relate translational wave func-

tions and derivatives between the two surfaces $u_\gamma = 0$ and $u_\gamma = u_\gamma^f$, where u_γ^f is a point in the Cartesian region at which the interaction potential has become negligible. It is then necessary to determine the overlap matrix which matches the wave function between arrangement channels. We require the matrices $\mathbf{C}_1^J$ and $\mathbf{C}_2^J$ which satisfy

$$\bar{\mathbf{f}}^{\alpha J}(u_\alpha) = \mathbf{C}_1^J \bar{\mathbf{f}}^{\beta J}(u_\beta),$$
$$\frac{d}{du_\alpha}\bar{\mathbf{f}}^{\alpha J}(u_\alpha) = -\mathbf{C}_2^J \frac{d}{du_\beta}\bar{\mathbf{f}}^{\beta J}(u_\beta) \tag{11}$$

on a suitably chosen matching surface. Here $\bar{\mathbf{f}}$ refers to a vector of solutions labeled by *adiabatic* states which are obtained by diagonalizing the close-coupling matrix at the matching surface in entrance or exit channel coordinates.

For the case of a "light–heavy–light" reaction, such as H + BrH, it is accurate to do the matching at $u_\alpha^0 = u_\beta^0 = 0$ as, to an excellent approximation,

$$\theta_\alpha = \theta_\beta = \theta \tag{12}$$

and the rotational basis set matches smoothly from entrance to exit channel. The discussion of matching matrices in the literature (see, for example, Refs. 50 and 52) usually involves the transformation of the "primitive" basis functions

$$Y_{j\Omega}(\theta_\gamma,\phi_\gamma)D^{J*}_{M\Omega}(\bar{\alpha},\bar{\beta},0)$$

between arrangement channels, and this transformation has a particularly simple form for light–heavy–light reactions (see Ref. 16). However, for symmetric light–heavy–light reactions such as H + BrH, the locally vibrationally-rotationally *adiabatic* basis functions for the α and β channels must match one-to-one at the matching surface, assuming $\theta_\alpha = \theta_\beta$ at $u_\alpha^0 = u_\beta^0 = 0$. Thus, in this exceptional case, the matching matrices $\mathbf{C}_1^J$ and $\mathbf{C}_2^J$ are equal to the identity matrix. Simplifications such as this have significant advantages in enabling small basis sets to be used in obtaining converged S matrix elements, and this is discussed further in Sec. III.

Once the global R matrix has been computed using the formulas of Ref. 48, the S matrix with elements

$$S^J_{nj\Omega n'j'\Omega'}$$

for the transition $nj\Omega \rightarrow n'j'\Omega'$ is obtained by applying the normal boundary conditions.[50] Differential and integral cross sections are then obtained from these S matrix elements by using standard formulas which are also discussed in Ref. 50.

An important simplification occurs in the solution of the CC equations since the (un-normalized) basis functions with definite parity

$$\left[D^{J*}_{M\bar{\Omega}}(\bar{\alpha},\bar{\beta},0)Y_{j\bar{\Omega}}(\theta_\gamma,\phi_\gamma) + pD^{J*}_{M-\bar{\Omega}}(\bar{\alpha},\bar{\beta},0)Y_{j-\bar{\Omega}}(\theta_\gamma,\phi_\gamma)\right] \tag{13}$$

can be used, where functions with $\bar{\Omega} \geqslant 0$ have even parity ($p = +1$) and those with $\bar{\Omega} < 0$ have odd parity ($p = -1$), and states with different parity do not mix in the close-coupled equations. Once the S matrices have been computed using these parity functions, it is straightforward[50] to transform the S matrix to the basis functions of Eq. (7). This transformation is necessary if differential cross sections are needed, but, if only integral cross sections averaged over initial m_j states and summed over final $m_{j'}$ states are of interest, then the formula

$$\sigma(n,j\rightarrow n',j') = \frac{\pi}{k^2_{nj}(2j+1)}\sum_J\sum_{\bar{\Omega}}\sum_{\bar{\Omega}'}\sum_p (2J+1)|S^{Jp}_{nj\bar{\Omega}n'j'\bar{\Omega}'}|^2 \tag{14}$$

can be used, where the S matrix is defined with respect to parity eigenfunctions and k_{nj} is the initial wave number. We note that[50]

$$\Omega = -m_j, \Omega' = m_{j'}$$

where the m_j projection quantum numbers are defined in the helicity representation in which the axis of quantization of the incoming and outgoing rotational states coincides with the direction of the incident and final wave vectors, respectively.

D. Comparison with ESA-CSA and IOSA methods

The details of the ESA-CSA method are described in Refs. 30–32. The technique follows that described in Sec. II except that the ESA is applied to the entrance reaction channel and the CSA is used for the exit reaction channel. Thus, in the entrance channel, the rotational angular momentum operator $\mathbf{j}_\alpha^2$ is replaced by the average value $\hbar^2\bar{j}(\bar{j}+1)$ where $\bar{j}$ is identified as an initial rotational quantum number. The coupled-channel expansion in the entrance channel has adiabatic vibrational functions multiplied by the orbital spherical harmonics of the form Y_{lK}. In the exit channel, the orbital angular momentum operator l_β^2 is replaced by the average value $\hbar^2\bar{l}(\bar{l}+1)$ and the rotational spherical harmonics Y_{jK} are used in the coupled-channel expansion. Here the quantum number K is the projection of the total angular momentum along the body-fixed Z axes which are directed along $\mathbf{r}_\alpha$ in the entrance channel, and along $\mathbf{R}_\beta$ for the exit channel. For light–heavy–light reactions, it is appropriate[53,54] to set $\bar{j} = \bar{l}$, and the wave functions in the entrance and exit channel match analytically since the relationships

$$\mathbf{R}_\alpha = \mathbf{r}_\beta, \mathbf{r}_\alpha = \mathbf{R}_\beta, \mathbf{j}_\alpha \equiv \mathbf{l}_\beta, \mathbf{j}_\beta \equiv \mathbf{l}_\alpha$$

hold. The S matrix elements obtained are $S^{\bar{J}K}_{nln'j'}$ and cross sections are computed from

$$\sigma(n,j\rightarrow n',j') = \frac{\pi}{k^2_{\bar{v}j}}\sum_K\sum_l |S^{\bar{J}K}_{nln'j'}|^2\,\delta_{\bar{j}j}. \tag{15}$$

In the IOSA, the ESA and CSA are applied together in both the entrance and exit reaction channels and the conditions $j = \bar{j}_\alpha = \bar{l}_\beta$ and $j' = \bar{l}_\alpha = \bar{j}_\beta$ are used.[17] The S matrix elements are now of the form

$$S^{jj'}_{nn'}(\theta),$$

and have to be computed for several values of θ using a purely vibrational basis set. The cross section expression is

$$\sigma(n,j\rightarrow n',j') = \frac{\pi}{k^2_{nj}}\frac{1}{2}(2j'+1)\int_0^\pi |S^{jj'}_{nn'}(\theta)|^2 \sin\theta\, d\theta. \tag{16}$$

Note that both the ESA-CSA and IOSA cross sections depend on the parameter $\bar{j}$ which only enters the dynamics calculations through the term

$$\frac{\bar{j}(\bar{j}+1)}{r_\gamma^2}. \tag{17}$$

Cross sections are not normally sensitive to this term in nonreactive calculations but they can be more sensitive in reaction calculations, as the average value of r_γ often stretches quite considerably at the reaction transition state, compared to its value in the asymptotic region. Thus, if $\bar{j}$ is chosen to be large, this term can contribute to a relative *decrease* in the effective energy barrier to reaction. This point is examined in some detail in Sec. IV.

It is valuable to compare the CC, ESA-CSA, and IOSA by comparing the cross section formulas, Eqs. (14)–(16). Thus the CC method requires a coupled basis set in n, j, and $\bar{\Omega}$ quantum numbers, and these calculations have to be repeated for many values of J and for even and odd parity p. The ESA-CSA couples n with j or ℓ, and these calculations have to be repeated for many values of K (but *not* for a range of J values), and the IOSA requires an expansion in n only, with computations required for many θ values. In practice, the computer time needed increases by an order of magnitude in going from IOSA to ESA-CSA, and in going from ESA-CSA to CC. Indeed, the CC calculations were only made possible by using the CRAY-1 computer with CRAY-vectorized subroutines being used for matrix multiplication, inversion, and diagonalization. Details on computer times are given in Sec. III.

III. NUMERICAL DETAILS

The numerical procedures used in our CC computations on the H + BrH→HBr + H reaction largely follow those described in our ESA-CSA computations.[30–33] A diatomics-in-molecules potential energy surface is used[31,55] which contains a three-center integral term which was parametrized by comparing ESA–CSA calculations with an experimental room temperature rate constant[43] for the D + BrH→DBr + H reaction. The adiabatic vibrational functions are calculated using the Cooley method[56] for $\theta_\gamma = 180°$, and all integrals involving these vibrational functions are calculated numerically. The potential energy surface, for a given value of $u_\gamma = u_\gamma^i$, is fitted to the form

$$A(v_\gamma) + B(v_\gamma)[1 + \cos\theta_\gamma],$$

with the functions A and B being determined by a fit to the potential at $\theta_\gamma = 180°$ and 170°. It was found that 128 R matrix sectors were sufficient to give converged cross sections to within 2%. The convergence of the results was also tested with respect to variation in the turning center of the curvilinear coordinate system and the CC basis set. The basis set is denoted by $(j_1 j_2,\ldots j_m ; N)$ where j_i refers to the number of different rotational basis states for adiabatic vibrational state i, and each of these j states has basis functions with the parity adapted projection quantum number $0,1,\ldots,N_m$ for even parity and $-1, -2,\ldots, -N_m$ for odd parity, where $|N_m|$ is the minimum value of j, J, and N. Over the energy range we studied (translational energies $E^j_{\rm Trans}$ ranging from threshold up to 0.29 eV), the largest basis set needed was (16,10,6,2;3) for a total energy of 0.45 eV. This particular calculation needed J values up to 16 to converge the cross sections, including even and odd parity, and a total of 3376 s of CRAY-1 CPU time was used. For lower energies, less cpu time was required; for example, with $E_{\rm Tot} = 0.26$ eV, 1209 s was needed. The relatively small value of N required is due to the strong anisotropy of the collinearly dominated potential; the reaction cross sections decrease considerably as $\bar{\Omega}$ increases.

TABLE I. Convergence test on CC calculations of $\sigma(j)(a_0^2)$ cross sections for the H + BrH reaction. $E_{\rm Tot} = 0.22$ eV.

j	Basis A[a]	Basis B[b]
0	0.758(−4)[c]	0.753(−4)
1	0.599(−4)	0.594(−4)
2	0.358(−4)	0.355(−4)
3	0.162(−4)	0.161(−4)
4	0.530(−5)	0.526(−5)
5	0.111(−5)	0.111(−5)
6	0.121(−6)	0.120(−6)

[a] Basis set A is (12, 8, 6;1). (49 basis functions for $J \geq 1$.)
[b] Basis set B is (14, 10, 5, 2;2). (81 basis functions for $J \geq 2$.)
[c] Numbers in parentheses are powers of ten.

Table I shows a convergence test, with respect to basis set size, on the CC computations of the integral cross sections

$$\sigma(j \to j') = \sigma(n = 0, j \to n' = 0, j').$$

On the evidence of tests such as this, we consider our reaction cross sections to be converged, with respect to basis set size, to within 5% for total energies of 0.38 eV and below, and to within 10% for total energies above 0.38 eV. Note

TABLE II. Cross sections $\sigma(j)$ for the H + BrH reaction calculated using the CC method. Units are a_0^2.

$E_{\rm Tot}$ (eV)	j								
	0	1	2	3	4	5	6	7	8
0.19	0.39(−5)[a]	0.28(−5)	0.15(−5)	0.55(−6)	0.15(−6)				
0.22	0.75(−4)	0.59(−4)	0.36(−4)	0.16(−4)	0.58(−5)	0.11(−5)	0.12(−6)		
0.26	0.95(−3)	0.76(−3)	0.52(−3)	0.29(−3)	0.13(−3)	0.44(−4)	0.10(−4)	0.19(−5)	0.16(−6)
0.30	0.85(−2)	0.73(−2)	0.54(−2)	0.34(−2)	0.18(−2)	0.81(−3)	0.29(−3)	0.76(−4)	0.16(−4)
0.34	0.38(−1)	0.35(−1)	0.29(−1)	0.21(−1)	0.13(−1)	0.75(−2)	0.34(−2)	0.12(−2)	0.35(−3)
0.38	0.14(+0)	0.13(+0)	0.11(+0)	0.89(−1)	0.65(−1)	0.42(−1)	0.23(−1)	0.12(−1)	0.42(−2)
0.42	0.45(+0)	0.42(+0)	0.37(+0)	0.32(+0)	0.25(+0)	0.19(+0)	0.13(+0)	0.77(−1)	0.38(−1)
0.45	0.65(+0)	0.64(+0)	0.62(+0)	0.57(+0)	0.51(+0)	0.44(+0)	0.34(+0)	0.23(+0)	0.14(+0)

[a] Numbers in parentheses are powers of ten.

TABLE III. Rate constants $k(T)$ for the H + BrH reaction in three dimensions. Units are $cm^3\ s^{-1}$ molecule^{-1}.

T/K	Method					
	ICVT[a]	ICVT-SCTSAG[a]	IOSA[b] ($\bar{j}=3$)	ESA-CSA[a] ($\bar{j}=3$)	ESA-CSA ($\bar{j}=0$)	CC
150	3.8(−19)[c]	4.0(−16)	5.0(−16)	3.4(−16)	2.2(−16)	1.3(−16)
200	3.2(−17)	1.7(−15)	1.9(−15)	1.5(−15)	1.1(−15)	7.6(−16)
250	4.7(−16)	6.0(−15)	6.4(−15)	5.6(−15)	4.2(−15)	3.4(−15)
300	2.9(−15)	1.7(−14)	1.8(−14)	1.6(−14)	1.3(−14)	1.1(−14)

[a] From Ref. 33.
[b] From Ref. 32.
[c] Numbers in parentheses are powers of ten.

that the translational energy is obtained from total energy by using

$$E^j_{\text{Trans}} = E_{\text{Tot}} - E_j,$$

where E_j is the energy of the HBr($v=0,j$) state, with $E_j = 0.162\,48$, $0.164\,58$, $0.168\,78$, $0.175\,08$, $0.183\,48$, $0.193\,98$, $0.206\,59$, $0.221\,29$, and $0.238\,09$ eV for $j = 0,1,...,7,8$, respectively.

Cross sections were calculated for eight total energies (for details see Sec. IV), and this was sufficient to give a converged room temperature rate constant $k(T)$ for temperatures up to 300 K. The rate constants were computed by fitting an exponential cubic spline function to the j selected cross sections,

$$\sigma(j) = \sum_{j'} \sigma(j \rightarrow j')$$

and the Maxwell–Boltzmann integral was then integrated numerically. The errors introduced by this numerical procedure for determining rate constants have been discussed before.[33] We did some extra ESA-CSA calculations for a larger range of energies to test the cubic spline procedure and found that this introduced an error no larger than 5%. Once the rate constants $k_j(T)$ had been computed using the CC cross sections, they were then Boltzmann-averaged to give $k(T)$. The convergence of this Boltzmann average over j was tested by having maximum values of $j = 7$ and 8 in the Boltzmann summation, and $k(T)$ only changed by 1%. Given the various convergence tests, it is difficult to give a highly accurate estimate of the total numerical error in $k(T)$, but our tests suggest that the reported values in Sec. IV are accurate to within 12%. It was not possible for us to estimate the errors introduced by the matching procedure we used and also by the neglect of the abstraction channel. In this regard, we note that our matching procedure is exact for a skew angle of 90°, and the skew angle for HBrH is 89.3°. Furthermore, the very strong bending potential should ensure that the effect of the abstraction channel on the exchange reaction is negligible.

IV. CALCULATIONS ON THE H + BrH REACTION

A. Cross sections and rate constants

Cross sections $\sigma(j)$, obtained in the CC computations on the H + BrH reaction, are presented in Table II. Results for eight different collisional energies are reported for $j = 0$-8. These cross sections were employed in calculating the rate constants $k_j(T)$ and $k(T)$ with the procedures described in Sec. III. Table III compares the CC $k(T)$ with those obtained using several other methods. Here ESA-CSA ($\bar{j}$) refers to the calculation[31–33] with the fixed initial value of $\bar{j}$, and results both for $\bar{j}=0$ and $\bar{j}=3$, the most highly populated rotational level at room temperature, are shown. Also presented in Table III are IOSA ($\bar{j}=3$) rate constants[32] and results computed[33] using two transition state theory methods.[41,42] These are the improved canonical variational transition state theory (ICVT) and the ICVT combined with a small curvature tunneling approximation and semiclassical adiabatic ground state transmission coefficient (SCTSAG).

As has been stated before,[32,33] the ICVT-SCTSAG, ESA-CSA ($\bar{j}=3$), and IOSA ($\bar{j}=3$) rate constants are in very good agreement, while the ICVT results are much too small as quantum tunneling is very important in this reaction at room temperature. It is interesting, however, that the CC $k(T)$ falls below the values obtained by the ICVT-SCTSAG, ESA-CSA ($\bar{j}=3$) and IOSA ($\bar{j}=3$) methods, although the agreement is good to within a factor of 2 at 250 K and above. This provides further evidence to suggest that the ICVT-SCTSAG approximation gives quite good results when tunneling is important, although the agreement with the CC results is not so spectacular as that obtained with the

TABLE IV. Rate constants k_j for the H + BrH (j) reaction in three dimensions. Units are $cm^3\ s^{-1}$ molecule^{-1}. The CC method is used.

T/K	j							
	0	1	2	3	4	5	6	7
150	1.8(−16)[a]	1.6(−16)	1.4(−16)	1.2(−16)	9.4(−17)	7.9(−17)	6.4(−17)	5.9(−17)
200	9.8(−16)	9.4(−16)	8.6(−16)	7.5(−16)	6.5(−16)	6.1(−16)	5.6(−16)	5.0(−16)
250	4.0(−15)	4.0(−15)	3.8(−15)	3.4(−15)	3.2(−15)	3.1(−15)	3.0(−15)	2.8(−15)
300	1.3(−14)	1.3(−14)	1.2(−14)	1.1(−14)	1.1(−14)	1.1(−14)	1.1(−14)	1.0(−14)

[a] Numbers in parentheses are powers of ten.

TABLE V. Comparison of ESA-CSA ($\bar{j}=0$) and CC cross sections $\sigma(j=0)$ for the H + BrH ($j=0$) reaction. Units are a_0^2.

E^0_{Trans} (eV)	ESA-CSA ($\bar{j}=0$)	CC ($j=0$)
0.0575	0.98(−4)[a]	0.75(−4)
0.0975	0.11(−2)	0.95(−3)
0.138	0.81(−2)	0.85(−2)
0.178	0.44(−1)	0.38(−1)
0.218	0.15(+0)	0.14(+0)
0.258	0.34(+0)	0.45(+0)

[a] Numbers in parentheses are powers of ten.

less accurate ESA-CSA ($\bar{j}=3$) method. The comparison of CC and ICVT/SCTSAG 3*D* rate constants is very similar to that obtained for the collinear reaction.[33] Thus the CC to ICVT/SCTSAG rate constant ratio for the collinear H + BrH reaction is 0.58 at 200 K and 0.83 at 300 K,[33] while the corresponding 3*D* ratios are 0.44 at 200 K and 0.65 at 300 K. We note also that Garrett and Truhlar have recently described[57] an alternative tunneling method to the small curvature tunneling approximation, and when tunneling is treated accurately in their approach the SCTSAG transmission coefficient is reduced by factors of 0.83 at 200 K and 0.93 at 300 K (see Table II of Ref. 57). This would bring their rate constants a little closer to our CC results, but the agreement would still not be perfect.

In the previous IOSA and ESA-CSA computations,[32,33] we set $\bar{j}=3$ as this is the most likely j state to be populated at room temperature. However, as was stated in Sec. II, since the average value of r_γ is larger at the transition state than its asymptotic value, then the effective activation energy will be decreased directly in the ESA-CSA and IOSA computations if $\bar{j}$ is nonzero. In the CC calculations, this will enter indirectly in the close–coupling matrix elements, but the effect will be largely averaged out by the large anisotropy in the potential upon diagonalization of the close-coupling matrix. To remove this effect, the ESA-CSA computations of rate constants were repeated for $\bar{j}=0$. These results are also shown in Table III, and are seen to fall roughly between the ESA-CSA ($\bar{j}=3$) and CC $k(T)$. The results clearly suggest that, in IOSA and ESA computations on strongly anisotropic reactions such as H + BrH, the most appropriate value of the parameter $\bar{j}$ is 0.

This feature is examined further in Table IV, where the rotationally selected CC constants $k_j(T)$ are shown. The CC $k_j(T)$ for $j=0$ are very close to the ESA-CSA ($\bar{j}=0$) $k(T)$ reported in Table III. Table V shows the ESA-CSA ($\bar{j}=0$) and CC ($j=0$) cross sections for a range of energies, and the agreement is very good. As explained above, the ESA-CSA cross sections and rate constants increase as $\bar{j}$ is increased. It is seen from Table IV, however, that the $k_j(T)$ obtained in the CC computations show a *decrease* as j is increased, and this is particularly prominent at low temperatures. This effect is related to the strong anisotropy in the potential. As was stated in Sec. III, the main contribution to the reaction cross section comes from the projection quantum number $\Omega=0$, and this is illustrated clearly in Table VI where the cross sections

$$\bar{\sigma}(j,\bar{\Omega}\rightarrow j',\bar{\Omega}') = \frac{\pi}{k_{nj}^2}\sum_J (2J+1)\left[\left|S^{Jp=1}_{nj\bar{\Omega}n'j'\bar{\Omega}'}\right|^2 + \left|S^{Jp=-1}_{nj-\bar{\Omega}n'j'-\bar{\Omega}'}\right|^2\right] \quad (18)$$

are shown for a given energy. Similar propensities have been observed in CC calculations on the $H + H_2 \rightarrow H_2 + H$ reaction[1] and are due to the wave function, for $\bar{\Omega}>0$, having a node along the path of minimum potential energy (the collinear configuration). Note that the cross sections of Table VI show that the "J_z conserving" reaction propensity $\Omega\rightarrow\Omega$ is favored, and this justifies the application of J_z conserving approximations, in which no coupling between different Ω states is allowed in solving the coupled-channel equations, to reactions larger than $H + H_2$.

The rate constants $k_j(T)$ of Table IV, however, are clearly not proportional to $(2j+1)^{-1}$. This is because of the strong rotational-translational coupling which transfers energy during the collision from rotation to translation and hence enhances reaction cross sections before they are degeneracy-averaged by the $(2j+1)$ factor (see the results of Tables II and VI). In the CC computations on $H + H_2$, it was found that the cross sections decreased more significantly with increasing j than in the present case.[1] However, for H_2, the rotational levels are more widely spaced than in HBr and the $H + H_2$ potential energy surface is not nearly so anisotropic as that for H + BrH. Thus rotational-translational energy transfer will not be so significant in $H + H_2$ as it is in H + BrH. Clearly, the present reaction does show some similarities, and some differences, to the $H + H_2$ reaction and this justifies the effort in extending the CC computations to reactions more complicated than $H + H_2$.

Although the agreement between the ICVT-SCTSAG, IOSA, ESA-CSA, and CC methods is quite reasonable, the above results do show that, for the calculation of highly accurate rate constants, it is important to use methods which treat the initial rotational state correctly, giving a rate constant which can be labeled as $k_j(T)$. This state-selective ability is not treated properly in the ICVT-SCTSAG, IOSA, and ESA-CSA theories for j larger than 0, and it is likely that this is the main reason why these theories all slightly overestimate the value of $k(T)$.

TABLE VI. Cross sections $\sigma(j=1,\bar{\Omega}\rightarrow j',\bar{\Omega}')$ for the H + BrH reaction with $E^{j=1}_{\text{Trans}}=0.127$ eV. These cross sections have not been degeneracy averaged. [see Eq. (18)].

j'	$\bar{\Omega}'$	σ/a_0^2 ($\bar{\Omega}=0$)	σ/a_0^2 ($\bar{\Omega}=1$)
0	0	0.31(−1)	0.21(−4)
1	0	0.78(−1)	0.52(−4)
1	1	0.52(−4)	0.54(−3)
2	0	0.91(−1)	0.55(−4)
2	1	0.17(−3)	0.19(−2)
2	2	0.49(−5)	0.13(−3)
3	0	0.75(−1)	0.41(−4)
3	1	0.26(−3)	0.34(−2)
3	2	0.15(−4)	0.50(−3)
3	3	0.30(−5)	0.22(−4)
4	0	0.46(−1)	0.25(−4)
4	1	0.25(−3)	0.40(−2)
4	2	0.28(−4)	0.98(−3)
4	3	0.17(−4)	0.94(−4)

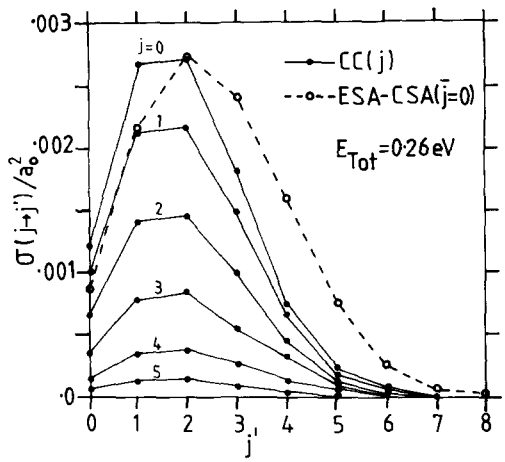

FIG. 1. Comparison of CC and ESA-CSA ($\bar{j} = 0$) calculations of cross sections $\sigma(j \to j')$ for the H + BrH→HBr + H reaction at $E_{\text{Tot}} = 0.26$ eV.

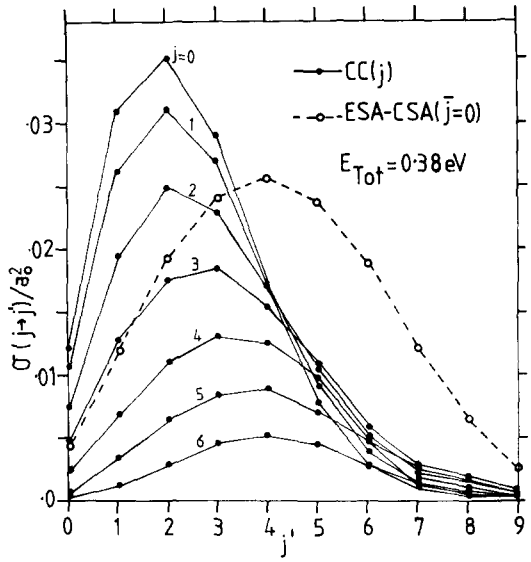

FIG. 2. Comparison of CC and ESA-CSA ($\bar{j} = 0$) calculations of cross sections $\sigma(j \to j')$ for the H + BrH→HBr + H reaction at $E_{\text{Tot}} = 0.38$ eV.

B. Rotational product distributions

The results discussed above largely refer to cross sections summed over the final HBr rotational state j'. Here we compare the CC computations of the cross sections $\sigma(j \to j')$ with those obtained using the ESA-CSA with $\bar{j} = 0$. We have pointed out before that the ESA-CSA and IOSA results for rotational distributions are in good agreement.[17,32] Figures 1 and 2 present the comparison of ESA-CSA and CC rotational cross sections for two different total energies and for several different values of initial j in the CC case. As is shown in Fig. 1, at the total energy of 0.26 eV the CC cross sections all peak at $j' = 2$, and so does the ESA-CSA distribution. However, the overall shape of the ESA-CSA distribution is different than the CC distributions, which are similar for all j. In particular, the ESA-CSA cross sections are too large at high j'. However, the j' *summed* ESA-CSA ($\bar{j} = 0$) cross sections agree well with the CC result for $j = 0$ (see Table V).

Figure 2 shows the rotational distributions for the higher total energy of 0.38 eV. Once again the CC distributions are quite similar for the different values of j. For $j = 0$, 1, and 2 the final state with the largest cross section is $j' = 2$, for $j = 3$ and 4 it is $j' = 3$ and, for $j = 5$ and 6, the distributions peak at $j' = 4$. In the ESA-CSA ($\bar{j} = 0$) computations, the rotational distribution peaks at $j' = 4$, and the cross sections for large j' are once again much greater in magnitude than the CC cross sections for all initial j. Overall, the ESA-CSA method cannot be claimed to be a highly accurate technique for computing rotational distributions. This must be due to the special sudden approximations used which involve the decoupling of rotational and total angular momentum, the accurate treatment of which is clearly needed for predicting reliable rotational distributions. This is despite the fact that the ESA-CSA method does use a coupled rotor expansion in the exit channel. The same criticism should be applied to the IOSA, which gives rotational distributions in excellent agreement with the ESA-CSA results.[32]

V. CONCLUSIONS

Close-coupling calculations of cross sections and rate constants have been performed on the H + BrH ($v = 0, j$)→HBr ($v = 0, j'$) + H reaction. Cross sections have been obtained for energies high enough to give a converged rate constant at room temperature. The results have been used to test the accuracy of those obtained using approximate theories, including sudden approximations (the ESA-CSA and IOSA) and an extended transition state theory with a tunneling correction. All of these approximate theories give rate constants in good agreement with each other, but the close-coupling rate constant $k(T)$ falls slightly below the approximate values. The difference is attributed to the fact that the rotationally selected rate constants $k_j(T)$ are quite sensitive to j, and none of the approximate theories is properly state selective in j. However, the rate constants are very sensitive to temperature in this reaction, for which tunneling is very important.

The results show that the most appropriate choice of the parameter $\bar{j}$, which arises in the ESA-CSA and IOSA methods, should be zero as this avoids any artificial lowering of the activation energy of the reaction which is due to bond stretching at the transition state. We have also found that the ESA-CSA and IOSA methods are not highly accurate techniques for yielding rotational product distributions for the H + BrH reactions.

The present results extend the existing data base of close-coupling results for cross sections and rate constants to a new class of reactions more complicated than H + H_2. We believe that the results presented here should have further use in testing the accuracy of approximate theories that are proposed for 3D reactions.

ACKNOWLEDGMENTS

This work was supported by the Science and Engineering Research Council. The calculations were performed on the CRAY-1 computer of the University of London Computer Centre.

[1] G. C. Schatz and A. Kuppermann, J. Chem. Phys. **65**, 4668 (1976).
[2] A. B. Elkowitz and R. E. Wyatt, J. Chem. Phys. **62**, 2504 (1975).

[3]R. B. Walker, E. B. Stechel, and J. C. Light, J. Chem. Phys. **69**, 2922 (1978).
[4]D. N. Neumark, A. M. Wodtke, G. N. Robinson, C. C. Hayden, and Y. T. Lee, ACS Symp. Ser. **263**, 479 (1984).
[5]M. Baer, Adv. Chem. Phys. **49**, 191 (1982).
[6]R. E. Wyatt, in *Atom–Molecule Collision Theory*, edited by R. B. Bernstein (Plenum, New York, 1979), Chap. 15.
[7]A. Kuppermann, G. C. Schatz, and J. P. Dwyer, Chem. Phys. Lett. **45**, 71 (1977).
[8]G. C. Schatz, Chem. Phys. Lett. **108**, 532 (1984).
[9]M. J. Redmon and R. E. Wyatt, Chem. Phys. Lett. **63**, 209 (1979).
[10]R. E. Wyatt and M. J. Redmon, Chem. Phys. Lett. **96**, 284 (1983).
[11]J. M. Bowman and K. T. Lee, J. Chem. Phys. **72**, 5071 (1980); **73**, 3522 (1980).
[12]V. Khare, D. J. Kouri, and M. Baer, J. Chem. Phys. **71**, 1188 (1979).
[13]D. J. Kouri, V. Khare, and M. Baer, J. Chem. Phys. **75**, 1179 (1981).
[14]J. Jellinek, M. Baer, V. Khare, and D. J. Kouri, Chem. Phys. Lett. **75**, 460 (1980).
[15]M. Baer, J. Jellinek, and D. J. Kouri, J. Chem. Phys. **78**, 2962 (1983).
[16]G. D. Barg and G. Drolshagen, Chem. Phys. **47**, 209 (1980).
[17]D. C. Clary and G. Drolshagen, J. Chem. Phys. **76**, 5027 (1982).
[18]K. T. Tang and M. Karplus, J. Chem. Phys. **49**, 1676 (1968); Phys. Rev. A **4**, 1844 (1971).
[19]W. H. Miller, J. Chem. Phys. **49**, 2373 (1968).
[20]R. B. Walker and R. E. Wyatt, J. Chem. Phys. **61**, 4839 (1974).
[21]B. H. Choi and K. T. Tang, J. Chem. Phys. **61**, 5147 (1974).
[22]J. C. Sun, B. H. Choi, R. T. Poe, and K. T. Tang, J. Chem. Phys. **78**, 4523 (1983).
[23]S. H. Suck, Phys. Rev. A **15**, 1983 (1977).
[24]S. H. Suck, Chem. Phys. Lett. **77**, 390 (1981).
[25]D. C. Clary and J. N. L. Connor, J. Chem. Phys. **75**, 3329 (1981).
[26]D. C. Clary and J. N. L. Connor, Mol. Phys. **41**, 689 (1981).
[27]D. C. Clary and J. N. L. Connor, Mol. Phys. **43**, 621 (1981).
[28]G. C. Schatz, L. M. Hubbard, P. S. Dardi, and W. H. Miller, J. Chem. Phys. **81**, 231 (1984).
[29]J. N. L. Connor and W. J. E. Southall, Chem. Phys. Lett. **108**, 527 (1984).
[30]D. C. Clary, Mol. Phys. **44**, 1067, 1083 (1981).
[31]D. C. Clary, Chem. Phys. **71**, 117 (1982).
[32]D. C. Clary, Chem. Phys. **81**, 379 (1983).
[33]D. C. Clary, B. C. Garrett, and D. G. Truhlar, J. Chem. Phys. **78**, 777 (1983).
[34]M. S. Child, Mol. Phys. **12**, 401 (1967).
[35]R. E. Wyatt, J. Chem. Phys. **51**, 3489 (1969).
[36]J. N. L. Connor and M. S. Child, Mol. Phys. **18**, 653 (1970).
[37]R. B. Walker and E. F. Hayes, J. Phys. Chem. **87**, 1255 (1983).
[38]E. F. Hayes and R. B. Walker, J. Phys. Chem. **88**, 3318 (1984).
[39]J. M. Bowman, G-Z. Ju, and K. T. Lee, J. Phys. Chem. **86**, 2232 (1982).
[40]J. M. Bowman, A. F. Wagner, S. P. Walch, and T. H. Dunning, J. Chem. Phys. **81**, 1739 (1984).
[41]D. G. Truhlar and B. C. Garrett, Acc. Chem. Res. **13**, 440 (1980).
[42]B. C. Garrett, D. G. Truhlar, and R. S. Grev, in *Potential Energy Surfaces and Dynamics Calculations*, edited by D. G. Truhlar (Plenum, New York, 1981), p. 587; D. G. Truhlar, A. D. Isaacson, R. T. Skodje, and B. C. Garrett, J. Phys. Chem. **86**, 2252 (1982); **87**, 4554(E); R. T. Skodje, D. G. Truhlar, and B. C. Garrett, J. Chem. Phys. **77**, 5955 (1982).
[43]H. Endo and G. P. Glass, J. Phys. Chem. **80**, 1519 (1976).
[44]J. D. McDonald and D. R. Herschbach, J. Chem. Phys. **62**, 4740 (1975).
[45]O. R. Wood and T. Y. Chang, Appl. Phys. Lett. **20**, 76 (1972).
[46]R. T Pack, J. Chem. Phys. **60**, 633 (1974).
[47]B. R. Johnson, Chem. Phys. Lett. **13**, 172 (1972).
[48]J. C. Light and R. B. Walker, J. Chem. Phys. **65**, 4272 (1976).
[49]M. E. Rose, *Elementary Theory of Angular Momentum* (Wiley, New York, 1957).
[50]G. C. Schatz and A. Kuppermann, J. Chem. Phys. **65**, 4642 (1976).
[51]J. C. Light and R. B. Walker, J. Chem. Phys. **65**, 1598 (1976).
[52]R. B. Walker, J. C. Light, and A. Altenberger-Siczek, J. Chem. Phys. **64**, 1166 (1976).
[53]M. Baer, Mol. Phys. **26**, 369 (1973).
[54]M. Baer and D. J. Kouri, J. Chem. Phys. **57**, 3441 (1976).
[55]I. Last and M. Baer, J. Chem. Phys. **75**, 288 (1981); I. Last (private communication).
[56]J. W. Cooley, Math. Comp. **15**, 363 (1961).
[57]B. C. Garrett and D. G. Truhlar, J. Chem. Phys. **79**, 4931 (1983).